C.P. No. 540



C.P. No. 540

MINISTRY OF AVIATION

*AERONAUTICAL RESEARCH COUNCIL*

*CURRENT PAPERS*

# A Method for Designing Body Shape to Produce Prescribed Pressure Distributions on Wing-Body Combinations at Supersonic Speeds

*by*

*J. G. Jones, B.A.*

LONDON: HER MAJESTY'S STATIONERY OFFICE

1961

SIX SHILLINGS NET

C.P. No.540

U.D.C. No.533.695.12:533.69.048.2:533.696:533.6.011.5

April, 1959

# A METHOD FOR DESIGNING BODY SHAPE TO PRODUCE PRESCRIBED PRESSURE DISTRIBUTIONS ON WING-BODY COMBINATIONS AT SUPERSONIC SPEEDS

by

J. G. Jones, B.A.

---

## SUMMARY

This note presents a numerical method, based on linearised quasi-cylinder theory, for designing body shape to produce prescribed pressures on body and wing in supersonic flow.

---

Previously issued as R.A.E. Tech. Note No. Aero 2607 - A.R.C. 21,341.

## LIST OF CONTENTS


| | | Page |
|---|---|---|
| 1 | INTRODUCTION | 4 |
| 2 | SUMMARY OF RESULTS OF QUASI-CYLINDER THEORY | 4 |
| 3 | DESIGN OF BODY SHAPE TO PRODUCE A PRESCRIBED PRESSURE DISTRIBUTION ON THE BODY | 6 |
| | 3.1 The integral equation | 6 |
| | 3.2 Numerical solution of the integral equation | 7 |
| | 3.3 Illustrative example | 9 |
| 4 | DESIGN OF BODY SHAPE TO PRODUCE A PRESCRIBED PRESSURE DISTRIBUTION AT SEVERAL SPANWISE WING STATIONS WITH VARIOUS ADDITIONAL PRESCRIBED CONSTRAINTS | 11 |
| | 4.1 Prescribed pressures at spanwise wing stations | 11 |
| | 4.1.1 The system of integral equations | 11 |
| | 4.1.2 Numerical solution of the system of integral equations | 14 |
| | 4.1.3 Illustrative example | 16 |
| | 4.2 Inclusion of prescribed pressures at stations on the body | 17 |
| | 4.3 Inclusion of constraints on the shape of the body | 18 |
| | 4.3.1 General remarks | 18 |
| | 4.3.2 Prescribed streamwise slope on body generators | 18 |
| | 4.3.3 Prescribed streamwise area distribution | 20 |
| | 4.4 Limitations on prescribed wing pressure distributions | 22 |
| 5 | LIFTING COMBINATIONS | 22 |
| | 5.1 Body parallel to free stream | 22 |
| | 5.2 Body at angle of attack | 23 |
| 6 | CONCLUSIONS | 23 |
| | LIST OF PRINCIPAL SYMBOLS | 24 |
| | LIST OF REFERENCES | 25 |
| | APPENDICES 1 - 2 | - |
| | TABLES 1 - 6 | - |
| | ILLUSTRATIONS - Figs.1-7 | - |
| | DETACHABLE ABSTRACT CARDS | - |

## LIST OF APPENDICES


| Appendix | | Page |
|---|---|---|
| 1 | Solution of the system of integral equations for small $\chi$ | 27 |
| 2 | Design of body shape with prescribed pressure and shape in the wing root | 30 |


## LIST OF TABLES


| Table | | |
|---|---|---|
| 1 | Numerical solution of integral equation using $\delta_1 = 0.1$ | 32 |
| 2 | Body shape for zero pressure coefficient on body in combination with wedge wing | 33 |
| 3 | Numerical solution of integral equation obtained using $\delta_1 = 0.1$ and $\delta_2 = 0.05$ | 34 |
| 4 | Prescribed pressure coefficients at spanwise wing stations | 35 |
| 5 | Numerical solution of the first system of integral equations | 35 |
| 6 | Numerical solution of the second system of integral equations | 36 |


## LIST OF ILLUSTRATIONS


| | Fig. |
|---|---|
| General arrangement | 1 |
| Rectangular wedge wing - circular cylindrical body combination | 2 |
| Pressure coefficient on the body due to the wing alone | 3 |
| Body shape for zero pressure coefficient on body in combination with wedge wing | 4 |
| Approximate pressures on cylindrical body in combination with wedge wing | 5 |
| Solution for body shape: step by step and series solutions | 6 |
| Combinations with antisymmetric body shaping | 7 |

## 1 INTRODUCTION

Body shaping may be used to obtain favourable interference between the wing and body of a wing-body combination. For example, it may be used to reduce wave drag, or to generate lift.

One way of designing the body shape is to design for prescribed pressures on the configuration.

The linearised wing-body interference theory of Nielsen[1,2] can be used to calculate the pressure field of a combination with a quasi-cylindrical shaped body at zero lift, or under special lifting conditions, in supersonic flow. In this paper a numerical method, based on Nielsen's theory, of solving the inverse problem, that is of finding the body shape required to produce prescribed pressures on body and wing is presented. The method is suitable for use with a desk calculating machine.

An advantage of designing body shape for prescribed pressures is that the effect of pressure gradients on the boundary layer can be taken into account. This approach has been used in Refs. 4, 5. Ref.5 describes methods that have been previously used to design body shape for a given pressure distribution: in this the pressure has been prescribed on a line in the wing root. The present paper extends the regions in which the pressure distribution can be prescribed. The method presented is in two parts. In the first (Section 3) the pressure distribution is prescribed on the body. In the second (Section 4) the pressure distribution is prescribed on several chordwise lines across the wing. In addition, the pressure distribution can be prescribed along a number of body generators, and subsidiary constraints on the body shape can be included.

Sections 2 to 4 are concerned with combinations with a horizontal plane of symmetry. Extensions to lifting combinations are described in Section 5.

## 2 SUMMARY OF RESULTS OF QUASI-CYLINDER THEORY

Nielsen's interference theory[1,2] applies to wing-body combinations employing bodies deviating only slightly in shape from a circular cylinder.

The body cross section at any x-position (Fig.1) is taken as a circle of radius unity on which are superimposed distortions that vary as cosines of even multiples of $\theta$ to preserve horizontal and vertical planes of symmetry.

Then the body radius, R, may be defined by

$$\frac{\partial R}{\partial x} = t \sum_{n=0}^{\infty} g_{2n}(x) \cos 2n\theta \qquad (1)$$

where $R \triangleq 1$ .

The velocity potential for the combination, $\phi_c$, can be written

$$\phi_c = \phi_w + \phi_i + \phi_d \qquad (2)$$

where $\phi_w$ is the potential of the wing alone,

$\phi_w + \phi_i$ is the potential for the corresponding undistorted combination,

and $\phi_d$ is the potential due to body distortions.

The pressure coefficient at any point of the combination can be written in corresponding form

$$P_c = P_{(w)} + P_{(i)} + P_{(d)} \qquad (3)$$

where

$$P_{(w)} = -\frac{2}{V}\frac{\partial \phi_w}{\partial x},$$

$$P_{(i)} = -\frac{2}{V}\frac{\partial \phi_i}{\partial x},$$

and

$$P_{(d)} = -\frac{2}{V}\frac{\partial \phi_d}{\partial x}.$$

The linearised expression, $-\frac{2}{V}\frac{\partial \phi}{\partial x}$, is adopted as pressure coefficient on both wing and body of the combination.

Then Nielsen shows that the pressure coefficient on the body due to body distortions is given by

$$P_{B(d)} = \frac{2t}{\beta}\sum_{n=0}^{\infty}\left[g_{2n}(x) - \frac{1}{\beta}\int_0^x g_{2n}(\xi)\, W_{2n}\left(\frac{x-\xi}{\beta}, 1\right) d\xi\right]\cos 2n\theta, \qquad (4)$$

where $W_{2n}(x,r)$ are 'influence functions' defined and tabulated in Ref.3.

The pressure coefficient on the wing due to body distortions is given by

$$P_{W(d)} = \frac{2t}{\beta}\sum_{n=0}^{\infty}\left[\frac{g_{2n}(x-\beta r+\beta)}{\sqrt{r}} - \frac{1}{\beta}\int_0^{x-\beta r+\beta} g_{2n}(\xi)\, W_{2n}\left(\frac{x}{\beta} - r + 1 - \frac{\xi}{\beta}, r\right) d\xi\right]$$

... (5)

## 3 DESIGN OF BODY SHAPE TO PRODUCE A PRESCRIBED PRESSURE DISTRIBUTION ON THE BODY

### 3.1 The integral equation

The pressure coefficient on the body is given, as in (3), by

$$P_B = P_{B(w)} + P_{B(i)} + P_{B(d)} \cdot \qquad (6)$$

$P_{B(w)} + P_{B(i)}$ is the pressure coefficient on the body of the corresponding combination with an unshaped cylindrical body. Nielsen shows how to find this in Ref.1. Provided no strong shock waves occur this pressure coefficient can also be found by experiment using an unshaped body.

So, if $P_B$ is prescribed then, indirectly, $P_{B(d)}$ is prescribed.

Suppose, then, we have

$$P_{B(d)} = P(x, \theta) \cdot \qquad (7)$$

Expanding $P(x, \theta)$ in a Fourier series and using (4)

$$\frac{2t}{\beta} \sum_{n=0}^{\infty} \left[ g_{2n}(x) - \frac{1}{\beta} \int_0^x g_{2n}(\xi)\, W_{2n}\left(\frac{x-\xi}{\beta}, 1\right) d\xi \right] \cos 2n\theta = P(x, \theta)$$

$$= \frac{2t}{\beta} \sum_{n=0}^{\infty} p_{2n}(x) \cos 2n\theta \cdot$$

... (8)

Equating Fourier coefficients, for all n,

$$\frac{1}{\beta} \left[ g_{2n}(x) - \frac{1}{\beta} \int_0^x g_{2n}(\xi)\, W_{2n}\left(\frac{x-\xi}{\beta}, 1\right) d\xi \right] = \frac{p_{2n}}{\beta}(x) \cdot \qquad (9)$$

Using Gothert's rule (as in Ref.2) a transformation is made to obtain an equivalent combination with $\beta = 1$.

Equation (9) then takes the form

$$g_{2n}(x) - \int_0^x g_{2n}(\xi)\, W_{2n}\left(x - \xi, 1\right) d\xi = p_{2n}(x) . \qquad (10)$$

This is a Volterra integral equation of the second kind for $g_{2n}(x)$.

The solution may be written

$$g_{2n}(x) = p_{2n}(x) + \int_0^x p_{2n}(\xi)\, S_{2n}(x-\xi, 1)\, d\xi$$

where $S_{2n}$ is the resolvent of $W_{2n}$, given[6] by

$$\begin{aligned} S_{2n}(x, 1) = {} & W_{2n}(x, 1) \\ & - \int_0^x W_{2n}(x-y_1, 1)\, W_{2n}(y_1, 1)\, dy_1 \\ & + \int_0^x W_{2n}(x-y_1, 1)\, dy_1 \int_0^{y_1} W_{2n}(y_1-y_2, 1)\, W_{2n}(y_2, 1)\, dy_2 \\ & - \ldots . \end{aligned}$$

Lock, in unpublished work, has obtained an integral expression in closed form for $S_o(x, 1)$ using operational methods, and has tabulated this function.

This paper avoids the necessity of tabulating the functions $S_{2n}(x, 1)$ by solving the integral equation (10) directly by numerical means.

3.2 Numerical solution of the integral equation

An approximation to the integral in (10) is made using the trapezium rule.

Equal intervals of length $\delta$ are taken along the x-axis.

Then we obtain the approximate equation

$$g_{2n}(\delta) \doteq p_{2n}(\delta) + \frac{\delta}{2}\left\{g_{2n}(0)\, W_{2n}(\delta, 1) + g_{2n}(\delta)\, W_{2n}(0, 1)\right\}.$$

Rearranging:

$$g_{2n}(\delta) \doteq \frac{p_{2n}(\delta) + \frac{\delta}{2} g_{2n}(0)\, W_{2n}(\delta, 1)}{1 - \frac{\delta}{2} W_{2n}(0, 1)}. \qquad (11)$$

Similarly there is obtained the general approximate formula

$$g_{2n}(m\delta) \doteq \frac{p_{2n}(m\delta) + \delta\left\{\frac{1}{2} g_{2n}(0)\, W_{2n}(m\delta, 1) + g_{2n}(\delta)\, W_{2n}(\overline{m-1}\,\delta, 1) + \ldots + g_{2n}(\overline{m-1}\,\delta)\, W_{2n}(\delta, 1)\right\}}{1 - \frac{\delta}{2} W_{2n}(0, 1)}.$$

... (12)

The step by step process is started by the equation (from (10)) $g_{2n}(0) = p_{2n}(0)$.

Using the above formula successive approximate values of $g_{2n}(\delta)$, $g_{2n}(2\delta)$, $g_{2n}(3\delta)$, ... can be calculated.

It is shown in Ref.11 that the error in this approximate method at any fixed value of x is $O(\delta^2)$.

Repeating the computation with interval length $\frac{\delta}{2}$ a check can be obtained on the accuracy of the solution with interval length $\delta$. Alternatively, the accuracy can be checked by evaluating the left hand side of (10) at several points using Simpson's Rule.

In most practical applications it is sufficient to compute about four Fourier components, $g_{2n}(x)$.

If the body shape is defined by

$$\frac{\partial R}{\partial x} = t \sum_{n=0}^{3} g_{2n}(x) \cos 2n\theta \qquad (13)$$

the pressure distribution produced is

$$2t \sum_{n=0}^{3} p_{2n}(x) \cos 2n\theta$$

whereas the prescribed pressure distribution is

$$2t \sum_{n=0}^{\infty} p_{2n}(x) \cos 2n\theta \qquad \text{(from (8))} .$$

The difference between these two quantities is in general small. A particular case of this is discussed in Section 3.3.

3.3 Illustrative example

Nielsen[1] has calculated the pressure distribution on a combination consisting of a rectangular wedge wing and a circular cylindrical body non-lifting configuration.

The arrangement is illustrated in Fig.2.

The total wedge angle is $2i_w$.

t is taken equal to $i_w$.

A body shape is now designed to produce a pressure coefficient on the body equal to zero.

Upstream of the wing leading edge the pressure coefficient on the body is equal to zero without shaping. The position of the wing leading edge is accordingly chosen as $x = 0$, and the body is shaped downstream of this point.

The case $\beta = 1$ is considered. Any other value of $\beta$ can be treated similarly.

Equation (6) now reduces to

$$P_{B(w)} + P_{B(i)} + P_{B(d)} = 0 .$$

Expanding in a Fourier series

$$2\, i_w \sum_{n=0}^{\infty} K_{2n}(x) \cos 2n\theta + 2\, i_w \sum_{n=0}^{\infty} L_{2n}(x) \cos 2n\theta + 2\, i_w \sum_{n=0}^{\infty} p_{2n}(x) \cos 2n\theta = 0 .$$

Equating Fourier coefficients

$$p_{2n}(x) = - K_{2n}(x) - L_{2n}(x), \qquad \text{for} \quad n = 0, 1, 2, \ldots . \tag{14}$$

The function $P_{B(w)}$ is illustrated in Fig.3.

The functions $L_{2n}(x)$ are illustrated in Ref.1 for n = 0, 1, 2, 3.

The functions $p_{2n}(x)$, obtained in this way from (14) are included in Table 1 for n = 0, 1, 2, 3.

Using these values of $p_{2n}(x)$ the integral equation (10) is now solved using the approximate formula (12).

The functions $g_{2n}(x)$ obtained for n = 0, 1, 2, 3 using an interval $\delta_1 = 0.1$ are given in Table 1.

Integration of (13) gives

$$R = 1 + i_w \sum_{n=0}^{3} \cos 2n\theta \int_0^x g_{2n}(\xi)\, d\xi . \tag{15}$$

Resulting values of R obtained by approximating to the integral by the trapezium rule are given in Table 2 for $\theta = 0, \pi/6, \pi/3, \pi/2$ and are plotted in Fig.4.

Fig.5a illustrates the difference between the pressure coefficient in the wing root of the undistorted combination due to the first four Fourier components (which is cancelled by adding the first four Fourier components of body shaping) and that estimated by Nielsen[1] to be the exact root pressure coefficient. Fig.5b illustrates the pressure coefficient on the top generator of the body due to the first four Fourier components. The exact pressure coefficient remains equal to zero for values of x less than $\pi/2$. For values of x increasing above $\pi/2$ the exact pressure coefficient curve fairs rapidly into the curve of Fig.5b[1]. The large local differences between the exact pressure coefficient and that given by the first four terms of its Fourier expansion (e.g. at the wing root leading edge, x = 0 in Fig.5a) are due to the exact pressure coefficient having a discontinuity along a line with a component in the free stream direction.

For the case n = 0 results obtained by taking $\delta_1 = 0.1$ and $\delta_2 = 0.05$ are presented in Table 3. The results agree to three decimal places over the range considered. For higher values of n, $W_{2n}(x, 1)$ oscillates more rapidly and smaller interval lengths have to be taken to obtain the same accuracy.

The amount of body shaping is directly proportional to $i_w$ (equation (15)). The shape must be kept within the limits of quasi-cylindrical theory, thus imposing a limit on $i_w$.

## 4 DESIGN OF BODY SHAPE TO PRODUCE A PRESCRIBED PRESSURE DISTRIBUTION AT SEVERAL SPANWISE WING STATIONS, WITH VARIOUS ADDITIONAL PRESCRIBED CONSTRAINTS

### 4.1 Prescribed pressures at spanwise wing stations

#### 4.1.1 The system of integral equations

The pressure coefficient on the wing is given as in (3) by

$$P_w = P_{w(w)} + P_{w(i)} + P_{w(d)} . \tag{16}$$

$P_w$ is prescribed.

$P_{w(w)} + P_{w(i)}$ is the pressure coefficient on the wing of the corresponding unshaped combination. Nielsen shows how to find this in Ref.1.

So, indirectly, $P_{w(d)}$ is prescribed.

As in Section 3, Gothert's rule is used to transform to the case $\beta = 1$.

Suppose, for example, pressure coefficients are prescribed on the wing for $r = r_0, r_1, r_2$.

In this case the body shape is taken to be defined by the equation

$$\frac{\partial R}{\partial x} = t \sum_{n=0}^{2} g_{2n}(x) \cos 2n\theta . \tag{17}$$

Then (from (5))

$$P_{w(d)} = 2t \sum_{n=0}^{2} \left[ \frac{g_{2n}(x-r+1.)}{\sqrt{r}} - \int_0^{x-r+1} g_{2n}(\xi)\, W_{2n}(x-r+1-\xi, r)\, d\xi \right] . \tag{18}$$

Writing $\chi = x - r + 1$ this becomes

$$P_{w(d)} = 2t \sum_{n=0}^{2} \left[ \frac{g_{2n}(\chi)}{\sqrt{r}} - \int_{o}^{\chi} g_{2n}(\xi)\, W_{2n}(\chi - \xi,\, r)\, d\xi \right]. \qquad (19)$$

$\chi$ is the distance downstream of the mach line which is the upstream limit of the pressure field due to body distortion.

Suppose the prescribed values of $P_{w(d)}$ at the stations $r = r_o, r_1, r_2$ are given respectively by $tP_o$, $tP_1$, $tP_2$, all defined as functions of $\chi$.

Then, from (19),

$$\left.\begin{aligned}
\sum_{n=0}^{2} \left[ \frac{g_{2n}(\chi)}{\sqrt{r_o}} - \int_{o}^{\chi} g_{2n}(\xi)\, W_{2n}(\chi - \xi,\, r_o)\, d\xi \right] &= \frac{P_o(\chi)}{2} \\
\sum_{n=0}^{2} \left[ \frac{g_{2n}(\chi)}{\sqrt{r_1}} - \int_{o}^{\chi} g_{2n}(\xi)\, W_{2n}(\chi - \xi,\, r_1)\, d\xi \right] &= \frac{P_1(\chi)}{2} \\
\sum_{n=0}^{2} \left[ \frac{g_{2n}(\chi)}{\sqrt{r_2}} - \int_{o}^{\chi} g_{2n}(\xi)\, W_{2n}(\chi - \xi,\, r_2)\, d\xi \right] &= \frac{P_2(\chi)}{2}
\end{aligned}\right\} \qquad (20)$$

The equations (20) form a system of Volterra integral equations for $g_{2n}(\chi)$, $n = 0, 1, 2$.

Some relations representing conditions governing compatible pressure distributions at different spanwise stations can be derived.

From (20)

$$\sum_{n=0}^{2} \left[ \frac{g_{2n}(0)}{\sqrt{r_o}} \right] = \frac{P_o(0)}{2}$$

with similar equations for $r = r_1, r_2$.

Hence

$$\sqrt{r_o}\, P_o(0) = \sqrt{r_1}\, P_1(0) = \sqrt{r_2}\, P_2(0) . \tag{21}$$

If the body shape is smooth, then

$$\left.\frac{dR}{dx}\right]_{x=0} = 0 \qquad \text{for all } \theta, \text{ and so, from (17),}$$

$$g_{2n}(0) = 0 , \quad n = 0, 1, 2, \tag{22}$$

Thus (21) becomes

$$P_o(0) = P_1(0) = P_2(0) = 0 . \tag{23}$$

For this last case, (22), a relation between the initial gradients

$$\left.\frac{dP_i(\chi)}{d\chi}\right]_{\chi=0} , \quad i = 0, 1, 2,$$

can also be derived.

From (20), for small $\chi$,

$$\sum_{n=0}^{2} g_{2n}(\chi) + O(\chi^2) = \frac{\sqrt{r_o}\, P_o(\chi)}{2}$$

with similar equations for $r = r_1, r_2$.

Hence

$$\sqrt{r_o}\, P_o'(0) = \sqrt{r_1}\, P_1'(0) = \sqrt{r_2}\, P_2'(0) . \tag{24}$$

If $g_{2n}(0) \neq 0$ for some $n = 0, 1, 2$, then, from (17), $\frac{\partial R}{\partial x}$ is discontinuous at $x = 0$, and the body has a ridge, perpendicular to the stream, at $x = 0$.

4.1.2 Numerical solution of the system of integral equations

The system of equations (20) is solved by a numerical method analogous to that used in Section 3. Approximations to the integrals in (20) are made using the trapezium rule.

Equal intervals of length $\delta$ are taken along the x-axis.

Then we obtain the approximate equation

$$\sum_{n=0}^{2} \frac{g_{2n}(\delta)}{\sqrt{r_o}} \doteq \frac{P_o(\delta)}{2} + \sum_{n=0}^{2} \frac{\delta}{2} \left\{ g_{2n}(0)\, W_{2n}(\delta, r_o) + g_{2n}(\delta)\, W_{2n}(0, r_o) \right\}.$$

Rearranging

$$\sum_{n=0}^{2} g_{2n}(\delta) \left\{ \frac{1}{\sqrt{r_o}} - \frac{\delta}{2} W_{2n}(0, r_o) \right\} \doteq \frac{P_o(\delta)}{2} + \sum_{n=0}^{2} \frac{\delta}{2} g_{2n}(0)\, W_{2n}(\delta, r_o) \qquad (25)$$

with similar equations for $r = r_1, r_2$.

Similarly there is obtained the general approximate formula

$$\sum_{n=0}^{2} g_{2n}(m\delta) \left\{ \frac{1}{\sqrt{r_o}} - \frac{\delta}{2} W_{2n}(0, r_o) \right\} \doteq \frac{P_o(m\delta)}{2} + \sum_{n=0}^{2} \delta \left\{ \frac{1}{2} g_{2n}(0)\, W_{2n}(m\delta, r_o) + \right.$$

$$\left. g_{2n}(\delta)\, W_{2n}(m-1\ \delta, r_o) + \ldots + g_{2n}(m-1\ \delta)\, W_{2n}(\delta, r_o) \right\} \qquad (26)$$

with similar equations for $r = r_1, r_2$.

Denoting the right hand sides of these equations by $Q_o(m\delta)$, $Q_1(m\delta)$, $Q_2(m\delta)$, respectively

$$\left.\begin{aligned}
\sum_{n=0}^{2} g_{2n}(m\delta)\left\{\frac{1}{\sqrt{r_0}} - \frac{\delta}{2} W_{2n}(0, r_0)\right\} &\doteq Q_0(m\delta) \\
\sum_{n=0}^{2} g_{2n}(m\delta)\left\{\frac{1}{\sqrt{r_1}} - \frac{\delta}{2} W_{2n}(0, r_1)\right\} &\doteq Q_1(m\delta) \\
\sum_{n=0}^{2} g_{2n}(m\delta)\left\{\frac{1}{\sqrt{r_2}} - \frac{\delta}{2} W_{2n}(0, r_2)\right\} &\doteq Q_2(m\delta)
\end{aligned}\right\} \quad (27)$$

The coefficients on the left hand side are independent of m, and so the solution of the equations (27) can be written

$$g_{2n}(m\delta) \doteq A_{2n}\, Q_0(m\delta) + B_{2n}\, Q_1(m\delta) + C_{2n}\, Q_2(m\delta), \quad n = 0, 1, 2, \quad (28)$$

where $A_{2n}$, $B_{2n}$, $C_{2n}$ depend only on the coefficients on the left hand side of (27).

If the waisting is smooth, the step by step process is started by equation (22). If the waisting has a ridge line at $x = 0$ the values of $g_{2n}(0)$, $n = 0, 1, 2$ have to be found using a series solution of the equations (20) for small $\chi$. This is described in Appendix 1.

Using the formula (28) successive approximate values of $g_{2n}(\delta)$, $g_{2n}(2\delta)$, $g_{2n}(3\delta)$, ... can be calculated.

It is shown in Ref.11 that the error in this approximate method at any fixed value of x is $O(\delta^2)$. This is true whatever the number of chordwise stations.

For small $\delta$ the algebraic equations (27) are ill-conditioned[7]*. (A set of algebraic equations is said to be ill-conditioned when the determinant of the set is small compared with the individual terms of its expansion along any row or column.) This implies that more significant figures must be retained in the numerical solution of the equation than would otherwise be necessary. In fact the coefficients $A_{2n}$, ... in (28) are $O\left(\frac{1}{\delta}\right)$ and so if rounding errors are to be maintained less than some quantity E in $g_{2n}(m\delta)$ they must be maintained less than $E\delta$ in $Q_0(m\delta)$, ... .

The ill conditioning of the equations becomes worse if the difference between any two of $r_0$, $r_1$, $r_2$ is small.

*A method for removing the ill-conditioning is discussed in Ref.11.

Repeating the computation with interval length $\frac{\delta}{2}$ a check can be obtained on the accuracy of the first calculation, or, alternatively, the accuracy can be checked by evaluating the integrals on the left hand side of (20) at several points using Simpson's Rule. Both types of check are applied in the illustrative example.

4.1.3 Illustrative example

Pressure coefficients are prescribed at the wing stations r = 1, 2 by the equations

$$\left.\begin{aligned} \frac{P_o(\chi)}{2} &= \chi - 0.5\,\chi^2 \\ \frac{\sqrt{2}}{2} P_1(\chi) &= \chi - \chi^2 \end{aligned}\right\} \qquad (29)$$

The example is designed to illustrate the step by step process rather than to design a particularly useful body shape.

The equations (29) satisfy the conditions for smooth shaping, equations (23) and (24). $P_o(\chi)$ and $P_1(\chi)$ are presented in Table 4.

The body shape is defined by the equation

$$\frac{\partial R}{\partial x} = t\left\{g_o(x) + g_2(x)\cos 2\theta\right\}.$$

The equations corresponding to (28) for interval lengths $\delta_1 = 0.1$ and $\delta_2 = 0.05$ are respectively

$$\left.\begin{aligned} g_o(m\delta_1) &= -19.0385\, Q_o(m\delta_1) + 28.2843\, Q_1(m\delta_1) \\ g_2(m\delta_1) &= 20.0641\, Q_o(m\delta_1) - 28.2843\, Q_1(m\delta_1) \end{aligned}\right\}$$

and

$$\left.\begin{aligned} g_o(m\delta_2) &= -39.0506\, Q_o(m\delta_2) + 56.5685\, Q_1(m\delta_2) \\ g_2(m\delta_2) &= 40.0633\, Q_o(m\delta_2) - 56.5685\, Q_1(m\delta_2) \end{aligned}\right\}.$$

Values of $g_o(x)$, $g_2(x)$ corresponding to the interval lengths $\delta_1 = 0.1$ and $\delta_2 = 0.05$ are presented in Table 5.

A single check has been applied using Simpson's rule. Using values of $g_o(x)$, $g_2(x)$ corresponding to $\delta_2 = 0.05$ the expressions corresponding to the left hand sides of equation (20) have been evaluated at $\chi = 0.60$. The differences between the values obtained and the prescribed values of $\frac{P_o}{2}$, $\frac{P_1}{2}$ (Table 4) are not greater than 0.001.

The series solution for small $\chi$ of the system of equations, described in Appendix 1, is

$$\left.\begin{aligned} g_o(x) &= -0.06250x + O(x^2) \\ g_2(x) &= 1.06250x + O(x^2) \end{aligned}\right\} .$$

The values of $g_o'(0)$, $g_2'(0)$ obtained from this solution are illustrated in Fig.6. There is good agreement with the initial slopes obtained by the step by step process.

4.2 Inclusion of prescribed pressures at stations on the body

Pressures may be prescribed at $\theta$-wise stations on the body in addition to those prescribed at wing stations.

With body shape defined by

$$\frac{\partial R}{\partial x} = t \sum_{n=0}^{N} g_{2n}(x) \cos 2n\theta$$

the pressure coefficient on the body due to body distortion is given by (4), in the case $\beta = 1$, as

$$P_{B(d)} = 2t \sum_{n=0}^{N} \left[ g_{2n}(x) - \int_o^x g_{2n}(\xi)\, W_{2n}(x - \xi, 1)\, d\xi \right] \cos 2n\theta .$$

If $P_{B(d)}$ is prescribed for $\theta = \theta_i$, approximate algebraic equations analogous to (27) are obtained in the form

$$\sum_{n=0}^{N} g_{2n}(m\delta) \left\{ 1 - \frac{\delta}{2} W_{2n}(0, 1) \right\} \cos 2n\,\theta_i = Q_i(m\delta)$$

where

$$Q_i(m\delta) = \frac{1}{2}\left\{P_{B(d)}\right\}_{\theta=\theta_i} + \sum_{n=0}^{N} \delta \left\{\frac{1}{2} g_{2n}(0)\, W_{2n}(m\delta, 1) + g_{2n}(\delta)\, W_{2n}(\overline{m-1}\ \delta, 1) + \cdots + g_{2n}(\overline{m-1}\ \delta)\, W_{2n}(\delta, 1)\right\} \cos 2n\,\theta_i \,.$$

Since $W_{2n}(0, 1) = 0.5$, for all n, the algebraic equations can be written

$$\left\{1 - \frac{\delta}{4}\right\} \sum_{n=0}^{N} g_{2n}(m\delta) \cos 2n\,\theta_i = Q_i(m\delta) \,. \qquad (30)$$

The equations (30) can be used in conjunction with the equations (27) to determine the body shape. The resulting set of algebraic equations will be ill-conditioned if the pressure coefficients are prescribed at two or more wing stations.

## 4.3 Inclusion of constraints on the shape of the body

### 4.3.1 General remarks

In addition to prescribing pressures as previously described in this section, two sorts of constraint on the body shape can be imposed.

The first constraint is to prescribe the streamwise slope on one or more body generators. The second is to prescribe the streamwise area distribution of the body.

### 4.3.2 Prescribed streamwise slope on body generators

The body slope, $\frac{\partial R}{\partial x}$, is prescribed at $\theta$-wise body stations.

With body shape defined by

$$\frac{\partial R}{\partial x} = t \sum_{n=0}^{N} g_{2n}(x) \cos 2\,n\theta$$

equations are obtained of the form

$$\sum_{n=0}^{N} g_{2n}(m\delta) \cos 2n\,\theta_i = \frac{1}{t}\left[\frac{\partial R}{\partial x}\right]_{\theta=\theta_i} .$$

These equations can be used in conjunction with equations (27) or (30) to determine the body shape.

The method fails if pressure and slope are prescribed on the same generator for then the determinant of the resulting set of algebraic equations vanishes. An important example of this is the case of prescribed pressure and shape in the wing root and this is discussed in Appendix 2

As an illustrative example body shaping is designed to produce a prescribed pressure distribution in the wing root and to impose the restriction $\frac{\partial R}{\partial x} = 0$ on the top body generator*.

The body shape is defined by the equation

$$\frac{\partial R}{\partial x} = t\left\{g_o(x) + g_2(x) \cos 2\theta\right\} .$$

When

$$\theta = \frac{\pi}{2}, \quad \frac{\partial R}{\partial x} = 0 .$$

So

$$g_o(m\delta) - g_2(m\delta) = 0 . \tag{31}$$

The prescribed value of $P_{B(d)}$ in the root ($\theta = 0$) is taken to be $tP_o(x)$, where

$$P_o(x) = -2x .$$

Corresponding to (30)

$$\left\{1 - \frac{\delta}{4}\right\} \sum_{n=0}^{1} g_{2n}(m\delta) = Q_o(m\delta) \tag{32}$$

---

* This particular problem has been solved in Ref.5.

where

$$Q_o(m\delta) = -m\delta + \sum_{n=0}^{1} \delta \left\{ \frac{1}{2} g_{2n}(0)\, W_{2n}(m\delta, 1) + \right.$$

$$\left. + g_{2n}(\delta)\, W_{2n}(\overline{m-1}\ \delta, 1) + \cdots + g_{2n}(\overline{m-1}\ \delta)\, W_{2n}(\delta, 1) \right\} .$$

Equations (31) and (32) give

$$g_o(m\delta) = g_2(m\delta) = \frac{Q_o(m\delta)}{2\left(1 - \frac{\delta}{4}\right)} . \qquad (33)$$

The error in $g_{2n}(x)$ for a given value of x, obtained from (33), is $O(\delta^2)$; the equations are not ill-conditioned as they were in 4.1.2.

Values of $g_o(x) = g_2(x)$ corresponding to two interval lengths of $\delta_1 = 0.1$ and $\delta_2 = 0.05$ are presented in Table 6. A comparison suggests that the error in the values corresponding to $\delta_1 = 0.1$ is not more than 0.0005.

4.3.3 Prescribed streamwise area distribution

The ability to obtain prescribed pressures together with a prescribed streamwise area distribution implies that the methods described in this report can, in principle, be used in conjunction with 'area rule' design.

The body cross sectional area is given by

$$A(x) = \frac{1}{2} \int_0^{2\pi} R^2 \, d\theta .$$

With body shape defined by

$$\frac{\partial R}{\partial x} = t \sum_{n=0}^{N} g_{2n}(x) \cos 2n\theta , \qquad [\text{where } R \doteq 1]$$

we have

$$\frac{dA}{dx} = \int_0^{2\pi} R \frac{\partial R}{\partial x} \, d\theta$$

$$= t \sum_{n=0}^{N} g_{2n}(x) \int_0^{2\pi} \cos 2n\theta \, d\theta + O(t^2)$$

$$= 2\pi t \, g_o(x) + O(t^2) .$$

That is, neglecting $O(t^2)$, the only Fourier component of body shape to affect area distribution is the first. So the first Fourier component is determined by the prescribed area distribution, and the higher order components can be defined by the prescribed pressure distribution..

Suppose, for example, it is required to obtain a prescribed area distribution and a prescribed pressure distribution in the wing root.

The body shape is defined by

$$\frac{\partial R}{\partial x} = t \sum_{n=0}^{1} g_{2n}(x) \cos 2n\theta .$$

Taking

$$\frac{dA}{dx} = 2\pi t \, M(x) , \qquad x > 0 ,$$

and

$$\left[ P_{w(d)} \right]_{r=1} = t \, P_o(x) , \qquad x > 0,$$

where $M(x)$ and $P_o(x)$ are given functions, there is obtained

$$g_o(x) = M(x)$$

and, from (5), taking $\beta = 1$,

$$\sum_{n=0}^{1} \left[ g_{2n}(x) - \int_o^x g_{2n}(\xi)\, W_{2n}(x - \xi, 1)\, d\xi \right] = \frac{P_o(x)}{2} .$$

Hence

$$g_2(x) - \int_o^x g_2(\xi)\, W_2(x - \xi, 1)\, d\xi = \frac{P_o(x)}{2} - M(x) + \int_o^x M(x)\, W_o(x - \xi, 1)\, d\xi .$$

This is an integral equation for $g_2(x)$ of the type solved numerically in Section 3.2.

Thus $g_o(x)$ and $g_2(x)$, defining the body shape, can be obtained.

### 4.4 Limitations on prescribed wing pressure distributions

The body shape corresponding to a prescribed wing pressure distribution must satisfy the following conditions if the prescribed pressure distribution is to be achieved in practice.

Firstly, the resulting body must not deviate too much from the basic cylinder; otherwise the theory is not applicable.

Secondly, the configuration must be such that the pressure gradient is nowhere so adverse as to cause the boundary layer to separate. In particular, the pressure gradients on the body must be checked for each body shape.

No rigid rules can be laid down to ensure that the configuration corresponding to a prescribed pressure distribution satisfies these conditions. This is partly a matter of trial and error. However, it is important to realise that the effect of body distortions on the wing pressure distribution decreases with distance from the body. For example, for small $\chi$, to a first order approximation, the pressure distribution due to any Fourier component of body shaping falls off along a mach line as $1/\sqrt{r}$. This implies that if a sensible body shape is to be derived, the pressures due to body distortion prescribed on the wing must fall off with distance in roughly this fashion.

## 5 LIFTING COMBINATIONS

### 5.1 Body parallel to free stream

As for combinations with a horizontal plane of symmetry, the potential for the combination, $\phi_c$, can be written

$$\phi_c = \phi_w + \phi_i + \phi_d . \qquad (2)$$

The pressure coefficient on the combination can be written in corresponding form

$$P = P_{(w)} + P_{(i)} + P_{(d)} \qquad (3)$$

where $P_{(w)} + P_{(i)}$ is the pressure coefficient on the corresponding unshaped combination.

If the wing is non lifting, or has supersonic leading edges, $P_{(w)} + P_{(i)}$ can be found using Nielsen's interference theory. The problem of finding $P_{(w)} + P_{(i)}$ for lifting wings with subsonic leading edges is discussed in Ref.10.

$P_{(d)}$ is the pressure coefficient due to body distortions. Non-symmetric body distortions can be written as the sum of a symmetric part and an antisymmetric part; this Section is concerned with antisymmetric body distortions. These can be treated by the methods already described in the special cases in which the upper and lower halves of the flow field due to body shape are independent. The two halves are treated separately and body shape and corresponding pressure coefficients are expanded in Fourier series that contain only cosines of even multiples of $\theta$. Examples of combinations which can be treated in this way are illustrated in Fig.7 (a and b). Fig.7a illustrates a combination with supersonic leading edge wing; the upper and lower halves of the flow field due to body shape are independent in the shaded region. Fig.7b illustrates a combination with subsonic leading edge wing with the antisymmetric shaping started so far downstream that the flow field due to waisting lies entirely downstream of the subsonic leading edge.

If the leading edge of the wing is subsonic, and the flow fields above and below the wing due to body shaping are not independent (Fig.7c), then the methods developed in this paper are, strictly, not applicable. However, even in this case, there may well be examples where the interference between the upper and lower surfaces can be neglected, and useful results obtained in practice. Such an example has been described briefly by Lock and Rogers[8].

## 5.2 Body at angle of attack

It is shown in Ref.1 how the pressure distribution on a combination of wing and unshaped cylindrical body can be found when the body is at an angle of attack. Pressures on a corresponding wing and shaped body combination can therefore be prescribed, because, to the accuracy of linearised theory, the pressure field due to body shape is independent of body angle of attack.

# 6 CONCLUSIONS

A numerical method has been developed, based on the supersonic interference theory of Nielsen[1,2], which enables body distortions to be designed which produce prescribed pressure distributions on the body, or at several spanwise stations on the wing, of a wing-body combination at zero lift or under special lifting conditions. The numerical computations can be carried out on a desk calculating machine.

Illustrative examples have been presented of each type of problem. The first type reduces to the solution of a Volterra integral equation, the second to the solution of a system of such equations. In the examples considered

the errors due to the approximate method have been checked, and found small enough, by performing the calculations using intervals of different lengths in the step by step numerical procedure.

Work is proceeding to investigate the applications of the methods of this note to the design of body shapes for particular purposes, for example, the control of the flow near the body on swept wing-body combinations at low supersonic speeds with the purpose of postponing the drag rise.

---

## LIST OF PRINCIPAL SYMBOLS

| | |
|---|---|
| $g_{2n}(x)$ | amplitude of body distortion due to 2nth harmonic |
| $\left\{g_{2n}(x)\right\}_{\delta}$ | numerical solution for $g_{2n}(x)$ obtained using interval length $\delta$ |
| $i_w$ | semi wedge angle of rectangular wedge wing |
| $M$ | free stream Mach number |
| $\beta = \sqrt{M^2 - 1}$ | |
| $p_{2n}(x)$ | amplitude of 2nth harmonic of the pressure coefficient on the body due to body distortions |
| $K_{2n}(x)$ | amplitude of 2nth harmonic of the pressure coefficient on the body due to the wing alone |
| $L_{2n}(x)$ | amplitude of 2nth harmonic of the pressure coefficient on the body due to interference |
| $p_c$ | pressure coefficient on the combination |
| $p_{(w)}$ | pressure coefficient due to wing alone |
| $p_{(i)}$ | pressure coefficient due to interference |
| $p_{(d)}$ | pressure coefficient due to body distortions |
| $p_B$ | pressure coefficient on the body |
| $p_w$ | pressure coefficient on the wing |
| $R$ | body radius |
| $t$ | parameter for magnitude of body indentation |
| $V$ | free stream velocity |
| $W_{2n}(x, r)$ | influence function |

## LIST OF PRINCIPAL SYMBOLS (Contd)

| | |
|---|---|
| $x, y, z$ | co-ordinate axes with origin on axis of quasi-cylindrical body, x downstream |
| $r, \theta$ | polar co-ordinates in y, z plane |
| $\chi = x - \beta r + \beta$ | distance downstream of mach line from point $(-\beta, 0, o)$ in wing plane |
| $\phi_c$ | velocity potential for complete combination |
| $\phi_w$ | velocity potential for wing alone |
| $\phi_i$ | interference velocity potential |
| $\phi_d$ | velocity potential for distorted body |
| $A(x)$ | body cross sectional area |

---

## LIST OF REFERENCES


| No. | Author | Title, etc. |
|---|---|---|
| 1 | Nielsen, J.N. | Quasi-cylindrical theory of wing-body interference at supersonic speeds and comparison with experiment. NACA Rep. 1252, 1955. |
| 2 | Nielsen, J.N. | General theory of wave-drag reduction for combinations employing quasi-cylindrical bodies with an application to swept wing and body combinations. NACA TN 3722 June 24, 1955. |
| 3 | Nielsen, J.N. | Tables of characteristic functions for solving boundary value problems of the wave equation with application to supersonic interference. NACA TN 3873, February 1957. |
| 4 | Küchemann, D.<br>Hartley, D.E. | The design of swept wings and wing-body combinations to have low drag at transonic speeds. ARC.17.869, April, 1955. |
| 5 | Bagley, J.A. | Body design for low-drag swept-wing combinations at transonic speeds. Unpublished RAE Report. |
| 6 | Volterra, V. | Theory of functionals. 1931. |
| 7 | Hartree, D.R. | Numerical analysis. Oxford Univ. Press. 1952. |
| 8 | Lock, R.C.<br>Rogers, E.W.E. | Some preliminary experimental results on the effect of asymmetric body waisting on the drag due to lift of a swept-back wing at transonic speeds. NPL/Aero/328. May 1957. |

LIST OF REFERENCES (Contd)


| No. | Author | Title, etc. |
|---|---|---|
| 9 | Kopal | Numerical analysis.<br>Chapman and Hall. 1955. |
| 10 | Ferrari, C. | High speed aerodynamics and jet propulsion.<br>Vol. VII. Section C. |
| 11 | Jones, J.G. | On the numerical solution of convolution integral equations and systems of such equations.<br>(To be published in "Mathematics of Computation".) |

# APPENDIX 1

## SOLUTION OF THE SYSTEM OF INTEGRAL EQUATIONS FOR SMALL $\chi$

### 1 INTRODUCTION

A system of two equations for two unknown functions is considered.

In this case the equations (20) reduce to

$$\left.\begin{aligned} \sum_{n=0}^{1} \left[ \frac{g_{2n}(\chi)}{\sqrt{r_o}} - \int_o^{\chi} g_{2n}(\xi) W_{2n}(\chi-\xi,\, r_o)\, d\xi \right] &= \frac{P_o(\chi)}{2} \\ \sum_{n=0}^{1} \left[ \frac{g_{2n}(\chi)}{\sqrt{r_1}} - \int_o^{\chi} g_{2n}(\xi) W_{2n}(\chi-\xi,\, r_1)\, d\xi \right] &= \frac{P_1(\chi)}{2} . \end{aligned}\right\} \qquad (34)$$

The Taylor expansion for the $W_m(x,r)$ function is given in Ref.3 and begins

$$W_m(x,r) = W_m(0,r) + O(x) \qquad (35)$$

where

$$W_m(0,r) = \frac{1}{8\sqrt{r}} \left(3+\frac{1}{r}\right) + \frac{m^2}{2\sqrt{r}} \left(1-\frac{1}{r}\right) . \qquad (36)$$

### 2 BODY SHAPE WITH RIDGE LINE

Initial values, $g_o(0)$ and $g_2(0)$, from which to start the step by step process of Section 4.1.2 are to be found

Expanding in Taylor series:

$$\left.\begin{aligned} P_o(x) &= P_o(0) + P_o'(0)\, x + O(x^2) \\ P_1(x) &= P_1(0) + P_1'(0)\, x + O(x^2) \end{aligned}\right\} \qquad (37)$$

$$\left.\begin{aligned} g_o(x) &= g_o(0) + g_o'(0)\, x + O(x^2) \\ g_2(x) &= g_2(0) + g_2'(0)\, x + O(x^2) . \end{aligned}\right\} \qquad (38)$$

From (21)

$$\sqrt{r_o}\, P_o(0) = \sqrt{r_1}\, P_1(0) \qquad (39)$$

Substituting from (35) through to (39) in (34) gives

$$\frac{g_o(0) + g_o'(0)\,\chi}{\sqrt{r_o}} - g_o(0)\,W_o(0,r_o)\,\chi + \frac{g_2(0) + g_2'(0)\,\chi}{\sqrt{r_o}} - g_2(0)\,W_2(0,r_o)\,\chi$$

$$= \frac{P_o(0) + P_o'(0)\,\chi}{2} + O(\chi^2).$$

And

$$\frac{g_o(0) + g_o'(0)\,\chi}{\sqrt{r_1}} - g_o(0)\,W_o(0,r_1)\,\chi + \frac{g_2(0) + g_2'(0)\,\chi}{\sqrt{r_1}} - g_2(0)\,W_2(0,r_1)\,\chi$$

$$= \frac{\frac{\sqrt{r_o}}{\sqrt{r_1}}\,P_o(0) + P_1'(0)\,\chi}{2} + O(\chi^2)\,.$$

Equating coefficients of powers of $\chi$ in these equations

$$g_o(0) + g_2(0) = \frac{\sqrt{r_o}\,P_o(0)}{2} \qquad (40)$$

$$g_o'(0) - \sqrt{r_o}\,g_o(0)\,W_o(0, r_o) + g_2'(0) - \sqrt{r_o}\,g_2(0)\,W_2(0, r_o) = \frac{\sqrt{r_o}\,P_o'(0)}{2} \qquad \ldots\ (41)$$

$$g_o'(0) - \sqrt{r_1}\,g_o(0)\,W_o(0, r_1) + g_2'(0) - \sqrt{r_1}\,g_2(0)\,W_2(0, r_1) = \frac{\sqrt{r_1}\,P_1'(0)}{2}\,. \qquad \ldots\ (42)$$

Subtracting (72) from (71)

$$\left\{\sqrt{r_1}\,W_o(0,r_1) - \sqrt{r_o}\,W_o(0,r_o)\right\} g_o(0) + \left\{\sqrt{r_1}\,W_2(0,r_1) - \sqrt{r_o}\,W_2(0,r_o)\right\} g_2(0)$$

$$= \frac{\sqrt{r_o}}{2}\,P_o'(0) - \frac{\sqrt{r_1}}{2}\,P_1'(0)\,. \qquad (43)$$

Equations (40) and (43) can be solved for $g_o(0)$ and $g_2(0)$.

3 SMOOTH BODY SHAPE

$g_o'(0)$ and $g_2'(0)$ are to be found. An example of their use is given in Section 4.1.3.

From (22) : $$g_o(0) = g_2(0) = 0 \tag{44}$$

From (23) : $$P_o(0) = P_1(0) = 0 \tag{45}$$

From (24) : $$\sqrt{r_o}\, P_o'(0) = \sqrt{r_1}\, P_1'(0) . \tag{46}$$

Equating terms $O(\chi)$ in (34)

$$\frac{g_o'(0)}{\sqrt{r_o}} + \frac{g_2'(0)}{\sqrt{r_o}} = \frac{P_o'(0)}{2} . \tag{47}$$

Equating terms $O(\chi^2)$ in (34)

$$\frac{g_o''(0)}{2\sqrt{r_o}} + \frac{g_2''(0)}{2\sqrt{r_o}} - \frac{g_o'(0)}{2} W_o(0,r_o) - \frac{g_2'(0)}{2} W_2(0,r_o) = \frac{P_o''(0)}{4} \tag{48}$$

$$\frac{g_o''(0)}{2\sqrt{r_1}} + \frac{g_2''(0)}{2\sqrt{r_1}} - \frac{g_o'(0)}{2} W_o(0,r_1) - \frac{g_2'(0)}{2} W_2(0,r_1) = \frac{P_1''(0)}{4} . \tag{49}$$

From (48) and (49)

$$\left\{\frac{\sqrt{r_1}}{2} W_o(0,r_1) - \frac{\sqrt{r_o}}{2} W_o(0,r_o)\right\} g_o'(0) + \left\{\frac{\sqrt{r_1}}{2} W_2(0,r_1) - \frac{\sqrt{r_o}}{2} W_2(0,r_o)\right\} g_2'(0)$$

$$= \frac{\sqrt{r_o}\, P_o''(0)}{4} - \frac{\sqrt{r_1}\, P_1''(0)}{4} \tag{50}$$

Equations (47) and (50) can be solved for $g_o'(0)$ and $g_2'(0)$

---

# APPENDIX 2

## DESIGN OF BODY SHAPE WITH PRESCRIBED PRESSURE AND SHAPE IN THE WING ROOT

### 1 INTRODUCTION

It was indicated in Section 4.3.2 that the method there described for prescribing pressure distribution and body shape on several body generators fails if pressure and shape are prescribed on the same generator. It is shown in this Appendix how the equations can be solved numerically in this case. Restrictions on the prescribed functions are discussed.

### 2 SOLUTION OF THE EQUATIONS

Suppose the body shape is defined by the equation

$$\frac{\partial R}{\partial x} = t\left\{g_o(x) + g_2(x)\cos 2\theta\right\}. \qquad (51)$$

The prescribed shape and pressure in the wing root due to body distortion are denoted by the functions $tG(x)$ and $tP_o(x)$ respectively.

That is

$$\left[\frac{\partial R}{\partial x}\right]_{\theta=0} = tG(x), \qquad (x > 0), \qquad (52)$$

and

$$\left[P_{w(d)}\right]_{r=1} = tP_o(x), \qquad (x > 0). \qquad (53)$$

Then from equations (51) and (52)

$$g_o(x) + g_2(x) = G(x). \qquad (54)$$

And from equations (5) and (53), taking $\beta = 1$

$$\sum_{n=0}^{1}\left[g_{2n}(x) - \int_o^x g_{2n}(\xi)\, W_{2n}(x-\xi,1)\, d\xi\right] = \frac{P_o(x)}{2} \qquad (55)$$

Equations (54) and (55) form the system of equations to be solved. Substituting from (54) in (55) there is obtained

$$\int_o^x g_o(\xi)\left\{W_2(x-\xi,1) - W_o(x-\xi,1)\right\} d\xi = \frac{P_o(x)}{2} - G(x) + \int_o^x G(\xi)\, W_2(x-\xi,1)\, d\xi. \qquad (56)$$

In this integral equation for $g_0(\xi)$ the function in brackets (influence function) on the left hand side of (56) vanishes at the upper end of the interval of integration ($W_{2n}(0,1) = 0.5$, all n).

The equation cannot be solved by the method previously used in this report, i.e. by approximating to the integral by the trapezium rule and solving step by step.

However, a completely different numerical approach to the solution of equations such as (56) exists. This depends on the transformation of the integral equation to one with constant limits of integration (Fredholm equation). The method is described in detail in Ref.9. Essentially, it depends on replacing the unknown function by a polynomial which is determined by satisfying the equation at a finite number of points. The problem then reduces to the solution of a system of simultaneous linear algebraic equations; the number of algebraic equations is equal to the number of points at which the integral equation is satisfied. It has been verified in a particular case, by evaluating the left hand side of (56) using the trapezium rule where $g_0(\xi)$ is the solution obtained as described, that this method can be used to solve equation (56). Quite good accuracy was obtained by satisfying the equation at six points, in general the number of algebraic equations it is necessary to solve depends on the accuracy required and on the nature of the prescribed functions $P_0(x)$ and $G(x)$.

## 3 LIMITATIONS ON THE PRESCRIBED FUNCTIONS

It has been found by considering a particular example that if the resulting body slope on the top body generator $t\{g_0(x) - g_2(x)\}$ from equation (51) is of much greater magnitude than the prescribed slope in the wing root $t\{g_0(x) + g_2(x)\}$ values of the pressure coefficient due to body distortion occurring further out on the wing may be of correspondingly greater magnitude than the values prescribed in the wing root. In practical applications it will usually be required that, in general terms, the values of pressure coefficient due to body distortion are greatest in the wing root and decrease smoothly away from the body. Hence a necessary condition is that the solution $g_0(x)$ is not of much greater magnitude than the prescribed function $G(x) = g_0(x) + g_2(x)$. To fix ideas, suppose that $G(x)$ is prescribed first. Then, from (56), it follows that a solution $g_0(x)$ satisfying the above condition is only obtainable for suitably chosen prescribed functions $P_0(x)$. Thus for the method to be useful in a practical application the prescribed functions $G(x)$ and $P_0(x)$ must be compatible in this sense.

In any particular case to determine if the prescribed functions are compatible is largely a matter of trial.

---

TABLE 1

Numerical solution of integral equation using $\delta_1 = 0.1$

| x | $p_0(x)$ | $p_2(x)$ | $p_4(x)$ | $p_6(x)$ | $g_0(x)$ | $g_2(x)$ | $g_4(x)$ | $g_6(x)$ |
|---|---|---|---|---|---|---|---|---|
| 0.0 | 0.000 | 0.000 | 0.000 | 0.000 | 0.000 | 0.00 | 0.00 | 0.00 |
| 0.1 | -0.060 | -0.121 | -0.117 | -0.112 | -0.062 | -0.12 | -0.12 | -0.12 |
| 0.2 | -0.115 | -0.229 | -0.210 | -0.181 | -0.121 | -0.24 | -0.23 | -0.22 |
| 0.3 | -0.167 | -0.320 | -0.265 | -0.193 | -0.180 | -0.36 | -0.32 | -0.29 |
| 0.4 | -0.216 | -0.389 | -0.281 | -0.154 | -0.238 | -0.45 | -0.40 | -0.33 |
| 0.5 | -0.259 | -0.439 | -0.265 | -0.080 | -0.292 | -0.54 | -0.45 | -0.34 |
| 0.6 | -0.296 | -0.479 | -0.226 | +0.001 | -0.342 | -0.63 | -0.49 | -0.32 |
| 0.7 | -0.331 | -0.506 | -0.163 | +0.075 | -0.392 | -0.71 | -0.51 | -0.30 |
| 0.8 | -0.362 | -0.511 | -0.099 | +0.124 | -0.439 | -0.77 | -0.52 | -0.27 |
| 0.9 | -0.390 | -0.510 | -0.028 | +0.132 | -0.484 | -0.84 | -0.52 | -0.24 |
| 1.0 | -0.422 | -0.487 | +0.026 | +0.084 | -0.534 | -0.89 | -0.52 | -0.25 |
| 1.1 | -0.450 | -0.466 | +0.076 | +0.040 | -0.582 | -0.94 | -0.51 | -0.24 |
| 1.2 | -0.475 | -0.438 | +0.108 | +0.003 | -0.627 | -0.98 | -0.50 | -0.23 |
| 1.3 | -0.499 | -0.406 | +0.120 | -0.030 | -0.672 | -1.03 | -0.49 | -0.23 |
| 1.4 | -0.518 | -0.368 | +0.118 | -0.051 | -0.713 | -1.07 | -0.48 | -0.23 |
| 1.5 | -0.537 | -0.327 | +0.106 | -0.056 | -0.755 | -1.10 | -0.48 | -0.24 |
| 1.6 | -0.556 | -0.282 | +0.089 | -0.048 | -0.797 | -1.12 | -0.47 | -0.25 |
| 1.7 | -0.575 | -0.236 | +0.066 | -0.030 | -0.840 | -1.14 | -0.45 | -0.25 |
| 1.8 | -0.590 | -0.192 | +0.037 | -0.005 | -0.879 | -1.16 | -0.45 | -0.25 |
| 1.9 | -0.606 | -0.151 | +0.011 | +0.012 | -0.920 | -1.18 | -0.44 | -0.26 |
| 2.0 | -0.622 | -0.113 | -0.010 | +0.020 | -0.961 | -1.20 | -0.44 | -0.26 |
| 2.1 | -0.638 | -0.080 | -0.027 | +0.022 | -1.003 | -1.21 | -0.45 | -0.27 |
| 2.2 | -0.652 | -0.048 | -0.038 | +0.020 | -1.043 | -1.22 | -0.46 | -0.26 |
| 2.3 | -0.664 | -0.022 | -0.041 | +0.008 | -1.080 | -1.23 | -0.45 | -0.27 |
| 2.4 | -0.675 | +0.002 | -0.040 | -0.005 | -1.117 | -1.24 | -0.45 | -0.28 |
| 2.5 | -0.686 | +0.021 | -0.034 | -0.010 | -1.155 | -1.25 | -0.45 | -0.28 |
| 2.6 | -0.698 | +0.038 | -0.026 | -0.015 | -1.194 | -1.25 | -0.45 | -0.28 |
| 2.7 | -0.708 | +0.050 | -0.016 | -0.015 | -1.232 | -1.26 | -0.45 | -0.28 |
| 2.8 | -0.716 | +0.058 | -0.010 | -0.012 | -1.267 | -1.27 | -0.46 | -0.28 |
| 2.9 | -0.724 | +0.062 | +0.003 | -0.010 | -1.303 | -1.27 | -0.46 | -0.29 |
| 3.0 | -0.732 | +0.066 | +0.010 | 0.000 | -1.339 | -1.27 | -0.46 | -0.29 |

## TABLE 2

Body shape for zero pressure coefficient on body in combination with wedge wing

| x | $\frac{1-R}{i_w}$ $(\theta = 0)$ | $\frac{1-R}{i_w}\left(\theta = \frac{\pi}{6}\right)$ | $\frac{1-R}{i_w}\left(\theta = \frac{\pi}{3}\right)$ | $\frac{1-R}{i_w}\left(\theta = \frac{\pi}{2}\right)$ |
|---|---|---|---|---|
| 0.0 | 0.000 | 0.000 | 0.000 | 0.000 |
| 0.1 | 0.021 | -0.003 | 0.003 | -0.003 |
| 0.2 | 0.087 | -0.013 | 0.009 | -0.007 |
| 0.3 | 0.189 | -0.024 | 0.018 | -0.015 |
| 0.4 | 0.316 | -0.031 | 0.031 | -0.028 |
| 0.5 | 0.466 | -0.034 | 0.044 | -0.042 |
| 0.6 | 0.635 | -0.030 | 0.056 | -0.057 |
| 0.7 | 0.821 | -0.015 | 0.065 | -0.069 |
| 0.8 | 1.018 | 0.009 | 0.073 | -0.078 |
| 0.9 | 1.222 | 0.043 | 0.079 | -0.086 |
| 1.0 | 1.434 | 0.086 | 0.084 | -0.094 |
| 1.1 | 1.656 | 0.136 | 0.092 | -0.102 |
| 1.2 | 1.889 | 0.197 | 0.103 | -0.111 |
| 1.3 | 2.130 | 0.265 | 0.117 | -0.122 |
| 1.4 | 2.378 | 0.340 | 0.134 | -0.134 |
| 1.5 | 2.633 | 0.421 | 0.153 | -0.145 |
| 1.6 | 2.894 | 0.506 | 0.176 | -0.154 |
| 1.7 | 3.160 | 0.598 | 0.192 | -0.164 |
| 1.8 | 3.430 | 0.696 | 0.232 | -0.174 |
| 1.9 | 3.706 | 0.797 | 0.267 | -0.182 |
| 2.0 | 3.989 | 0.903 | 0.305 | -0.189 |
| 2.1 | 4.278 | 1.012 | 0.348 | -0.194 |
| 2.2 | 4.574 | 1.124 | 0.396 | -0.196 |
| 2.3 | 4.876 | 1.241 | 0.445 | -0.196 |
| 2.4 | 5.182 | 1.363 | 0.499 | -0.194 |
| 2.5 | 5.492 | 1.489 | 0.557 | -0.188 |
| 2.6 | 5.806 | 1.619 | 0.619 | -0.178 |
| 2.7 | 6.125 | 1.753 | 0.685 | -0.165 |
| 2.8 | 6.451 | 1.892 | 0.752 | -0.149 |
| 2.9 | 6.782 | 2.035 | 0.823 | -0.130 |
| 3.0 | 7.116 | 2.179 | 0.895 | -0.108 |

TABLE 3

Numerical solution of integral equation obtained using $\delta_1 = 0.1$ and $\delta_2 = 0.05$

| x | $g_0(x)$ ($\delta_1 = 0.1$) | $g_0(x)$ ($\delta_2 = 0.05$) |
|---|---|---|
| 0.00 | 0.0000 | 0.0000 |
| 0.05 | | -0.0304 |
| 0.10 | -0.0615 | -0.0615 |
| 0.15 | | -0.0913 |
| 0.20 | -0.1208 | -0.1208 |
| 0.25 | | -0.1520 |
| 0.30 | -0.1797 | -0.1796 |
| 0.35 | | -0.2100 |
| 0.40 | -0.2379 | -0.2380 |
| 0.45 | | -0.2643 |
| 0.50 | -0.2923 | -0.2924 |
| 0.55 | | -0.3183 |
| 0.60 | -0.3424 | -0.3424 |
| 0.65 | | -0.3673 |
| 0.70 | -0.3918 | -0.3917 |
| 0.75 | | -0.4126 |
| 0.80 | -0.4389 | -0.4386 |
| 0.85 | | -0.4640 |
| 0.90 | -0.4838 | -0.4839 |
| 0.95 | | -0.4986 |
| 1.00 | -0.5342 | -0.5337 |
| 1.05 | | -0.5583 |
| 1.10 | -0.5816 | -0.5813 |
| 1.15 | | -0.6031 |
| 1.20 | -0.6271 | -0.6262 |
| 1.25 | | -0.6488 |
| 1.30 | -0.6722 | -0.6716 |
| 1.35 | | -0.6926 |
| 1.40 | -0.7131 | -0.7130 |

TABLE 4

Prescribed pressure coefficients at spanwise wing stations

| $\chi$ | $\frac{P_o}{2} = \chi - 0.5\,\chi^2$ | $\frac{P_1}{2} = \frac{\chi - \chi^2}{\sqrt{2}}$ |
|---|---|---|
| 0.00 | 0.00000 | 0.00000 |
| 0.05 | 0.04875 | 0.03359 |
| 0.10 | 0.09500 | 0.06364 |
| 0.15 | 0.13875 | 0.09016 |
| 0.20 | 0.18000 | 0.11314 |
| 0.25 | 0.21875 | 0.13258 |
| 0.30 | 0.25500 | 0.14849 |
| 0.35 | 0.28875 | 0.16087 |
| 0.40 | 0.32000 | 0.16970 |
| 0.45 | 0.34875 | 0.17501 |
| 0.50 | 0.37500 | 0.17678 |
| 0.55 | 0.39875 | 0.17501 |
| 0.60 | 0.42000 | 0.16970 |
| 0.65 | 0.43875 | 0.16087 |
| 0.70 | 0.45500 | 0.14849 |
| 0.75 | 0.46875 | 0.13258 |
| 0.80 | 0.48000 | 0.11314 |
| 0.85 | 0.48875 | 0.09016 |
| 0.90 | 0.49500 | 0.06364 |
| 0.95 | 0.49875 | 0.03359 |
| 1.00 | 0.50000 | 0.00000 |

TABLE 5

Numerical solution of the first system of integral equations

| x | $g_o(x)$ | | $g_2(x)$ | |
|---|---|---|---|---|
| | $(\delta_1 = 0.1)$ | $(\delta_2 = 0.05)$ | $(\delta_1 = 0.1)$ | $(\delta_2 = 0.05)$ |
| 0.00 | 0.0000 | 0.0000 | 0.0000 | 0.0000 |
| 0.05 | | -0.0036 | | 0.0529 |
| 0.10 | -0.0086 | -0.0172 | 0.1061 | 0.1149 |
| 0.15 | | -0.0318 | | 0.1769 |
| 0.20 | -0.0547 | -0.0578 | 0.2459 | 0.2496 |
| 0.25 | | -0.0842 | | 0.3223 |
| 0.30 | -0.1131 | -0.1225 | 0.3961 | 0.4065 |
| 0.35 | | -0.1610 | | 0.4910 |
| 0.40 | -0.2067 | -0.2127 | 0.5810 | 0.5886 |
| 0.45 | | -0.2645 | | 0.6866 |
| 0.50 | -0.3182 | -0.3286 | 0.7849 | 0.7975 |
| 0.55 | | -0.3959 | | 0.9124 |
| 0.60 | -0.4654 | -0.4729 | 1.0272 | 1.0378 |
| 0.65 | | -0.5531 | | 1.1675 |
| 0.70 | -0.6338 | -0.6471 | 1.2951 | 1.3124 |
| 0.75 | | -0.7413 | | 1.4590 |
| 0.80 | -0.8382 | -0.8496 | 1.6050 | 1.6216 |
| 0.85 | | -0.9591 | | 1.7871 |
| 0.90 | -1.0685 | -1.0838 | 1.9484 | 1.9702 |
| 0.95 | | -1.2081 | | 2.1551 |
| 1.00 | -1.3339 | -1.3494 | 2.3362 | 2.3597 |

## TABLE 6

Numerical solution of the second system of integral equations

| x | $g_0(x) = g_2(x)$ ($\delta_1 = 0.1$) | $g_0(x) = g_2(x)$ ($\delta_2 = 0.05$) |
|---|---|---|
| 0.00 | 0.0000 | 0.0000 |
| 0.05 | | -0.0253 |
| 0.10 | -0.0513 | -0.0513 |
| 0.15 | | -0.0780 |
| 0.20 | -0.1055 | -0.1055 |
| 0.25 | | -0.1338 |
| 0.30 | -0.1630 | -0.1630 |
| 0.35 | | -0.1931 |
| 0.40 | -0.2242 | -0.2242 |
| 0.45 | | -0.2561 |
| 0.50 | -0.2890 | -0.2891 |
| 0.55 | | -0.3231 |
| 0.60 | -0.3582 | -0.3582 |
| 0.65 | | -0.3944 |
| 0.70 | -0.4315 | -0.4316 |
| 0.75 | | -0.4701 |
| 0.80 | -0.5093 | -0.5095 |
| 0.85 | | -0.5504 |
| 0.90 | -0.5917 | -0.5919 |
| 0.95 | | -0.6350 |
| 1.00 | -0.6788 | -0.6791 |



WT.2078.C.P.540.K3 - Printed in England

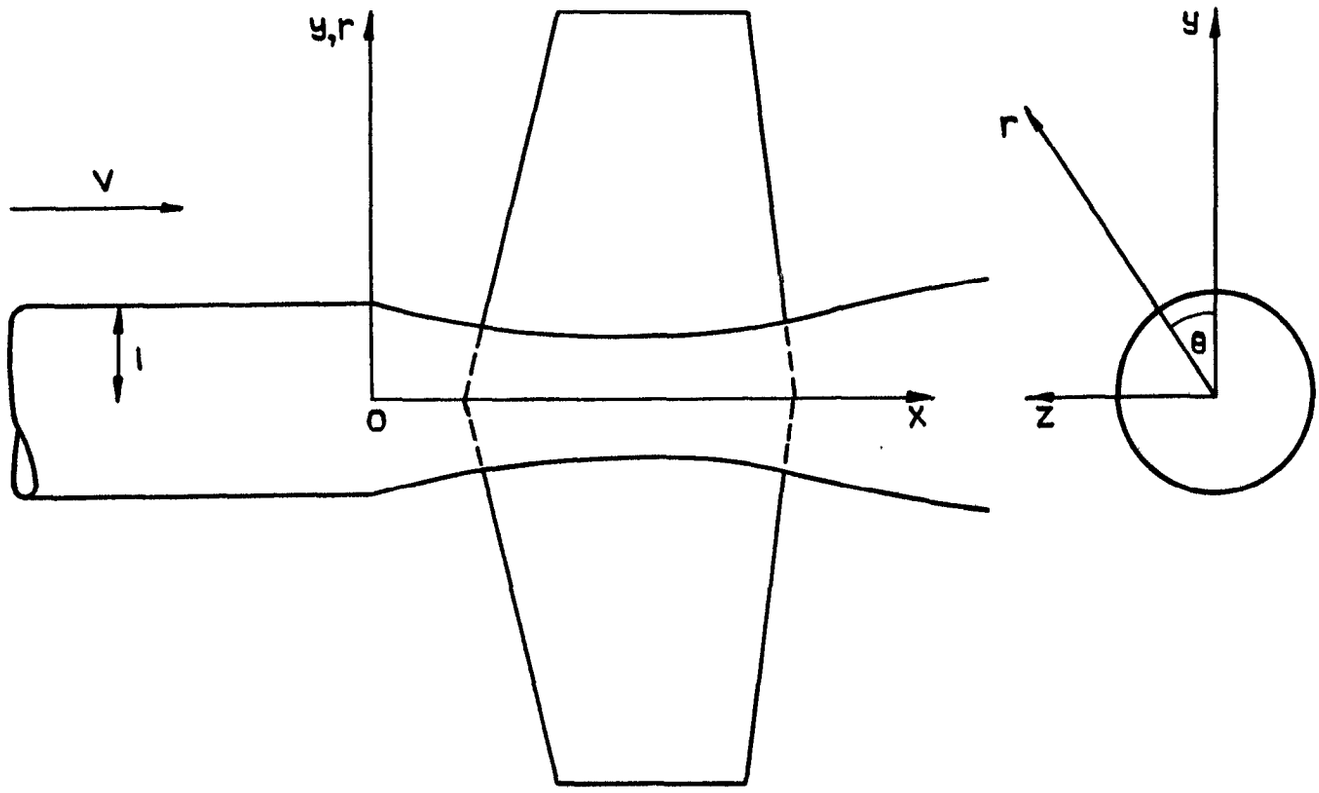


FIG. 1 GENERAL ARRANGEMENT.

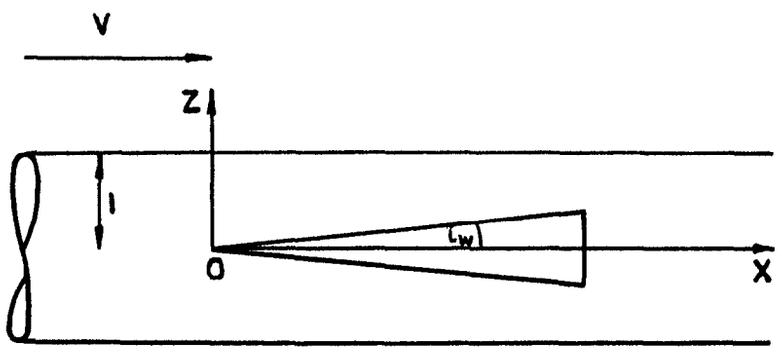


FIG. 2 RECTANGULAR WEDGE WING-CIRCULAR CYLINDRICAL BODY COMBINATION.

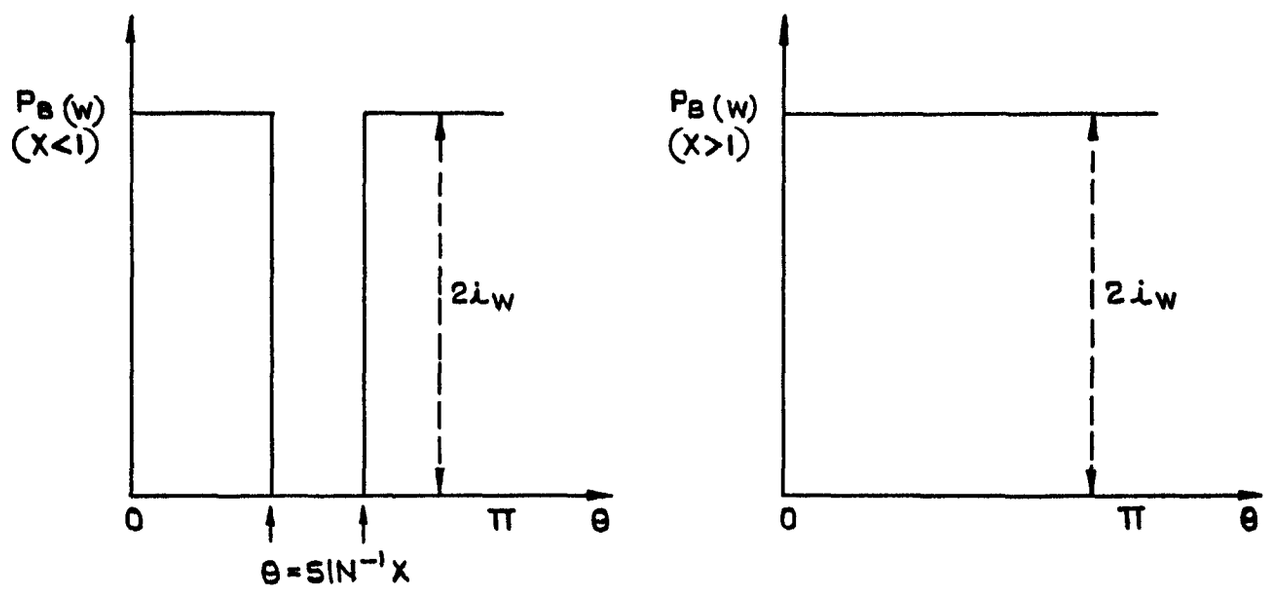


FIG.3 PRESSURE COEFFICIENT ON THE BODY DUE TO THE WING ALONE.

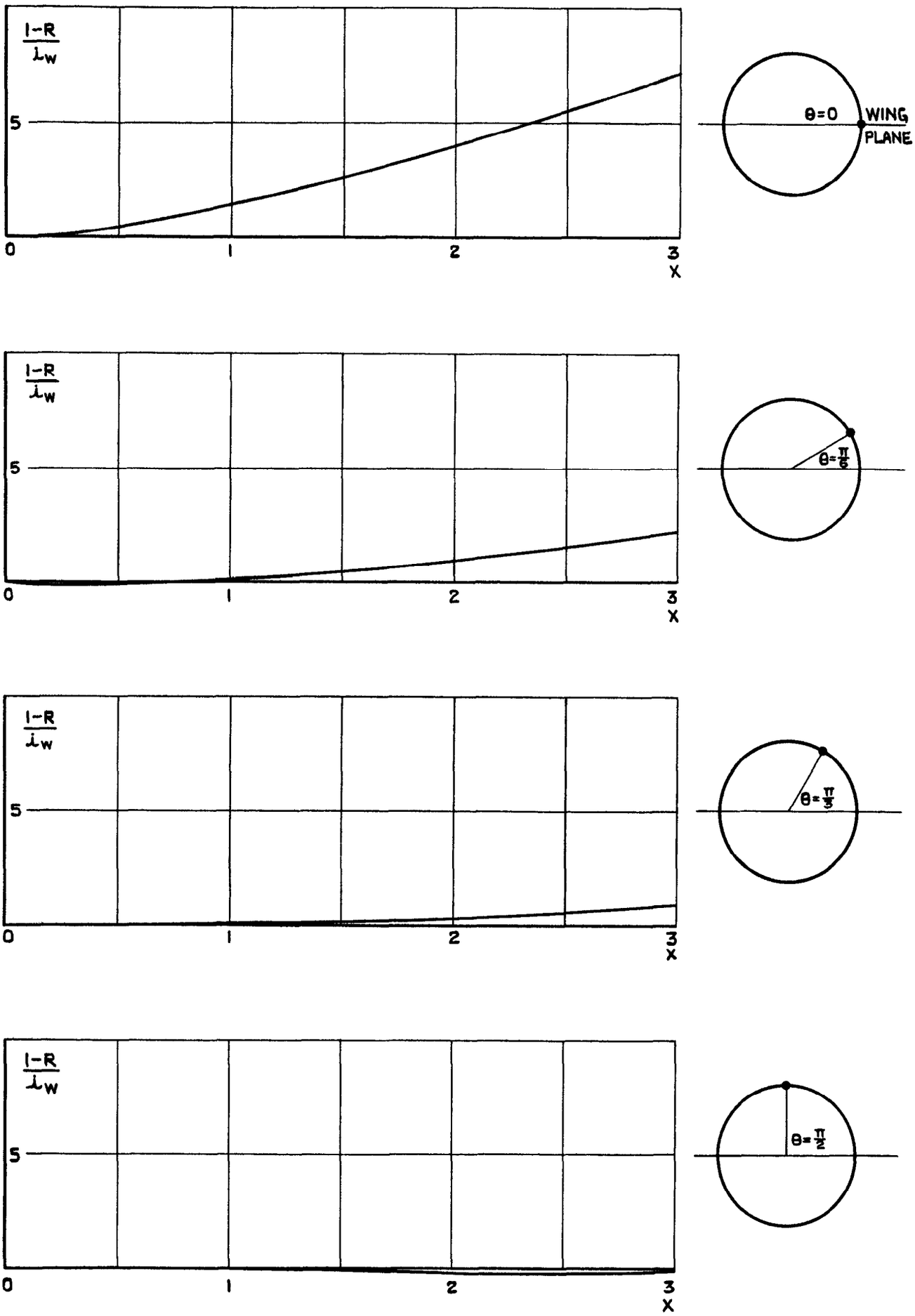


FIG. 4 BODY SHAPE FOR ZERO PRESSURE COEFFICIENT ON BODY IN COMBINATION WITH WEDGE WING.

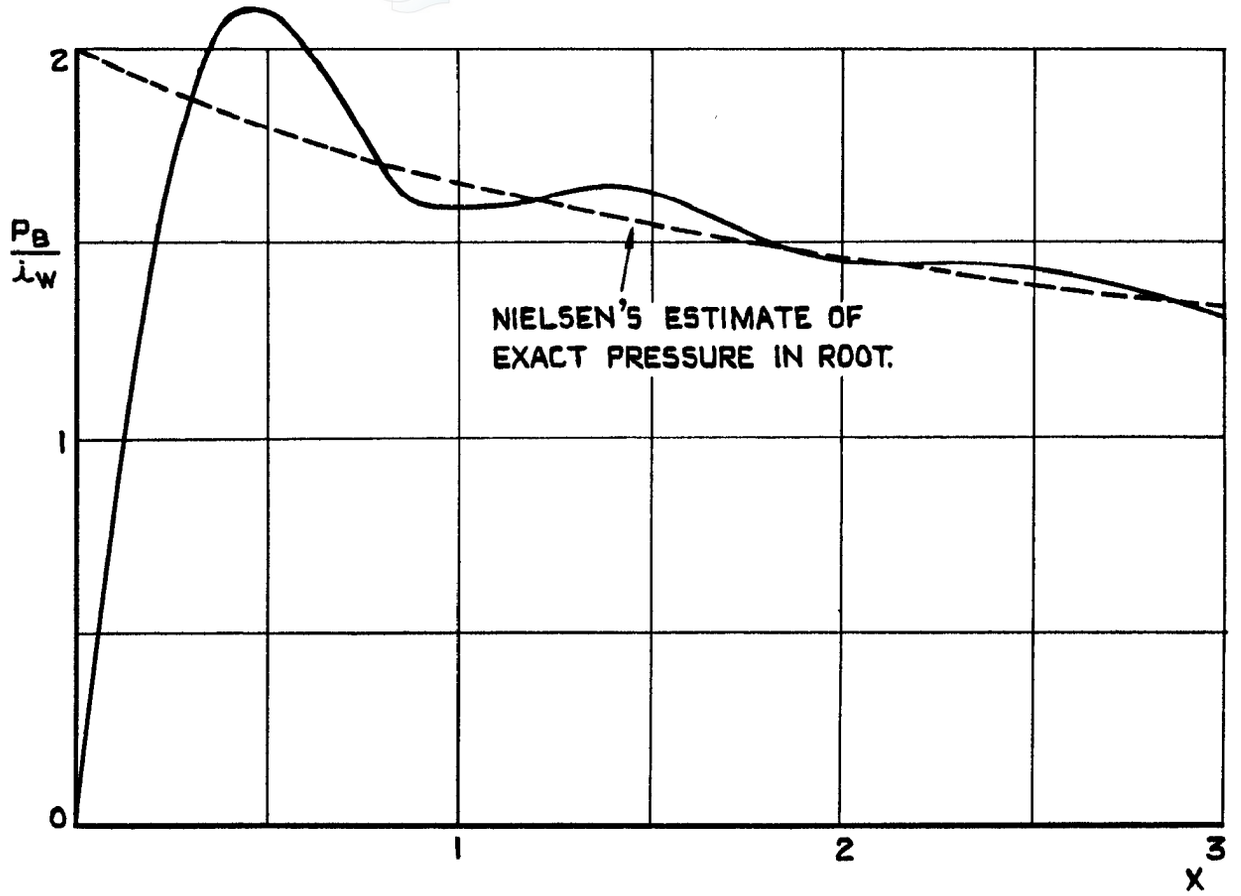


(a) APPROXIMATE PRESSURE IN WING ROOT GIVEN BY FIRST FOUR FOURIER COMPONENTS $\left(-2\sum_{0}^{3} p_{2n}(X)\right)$

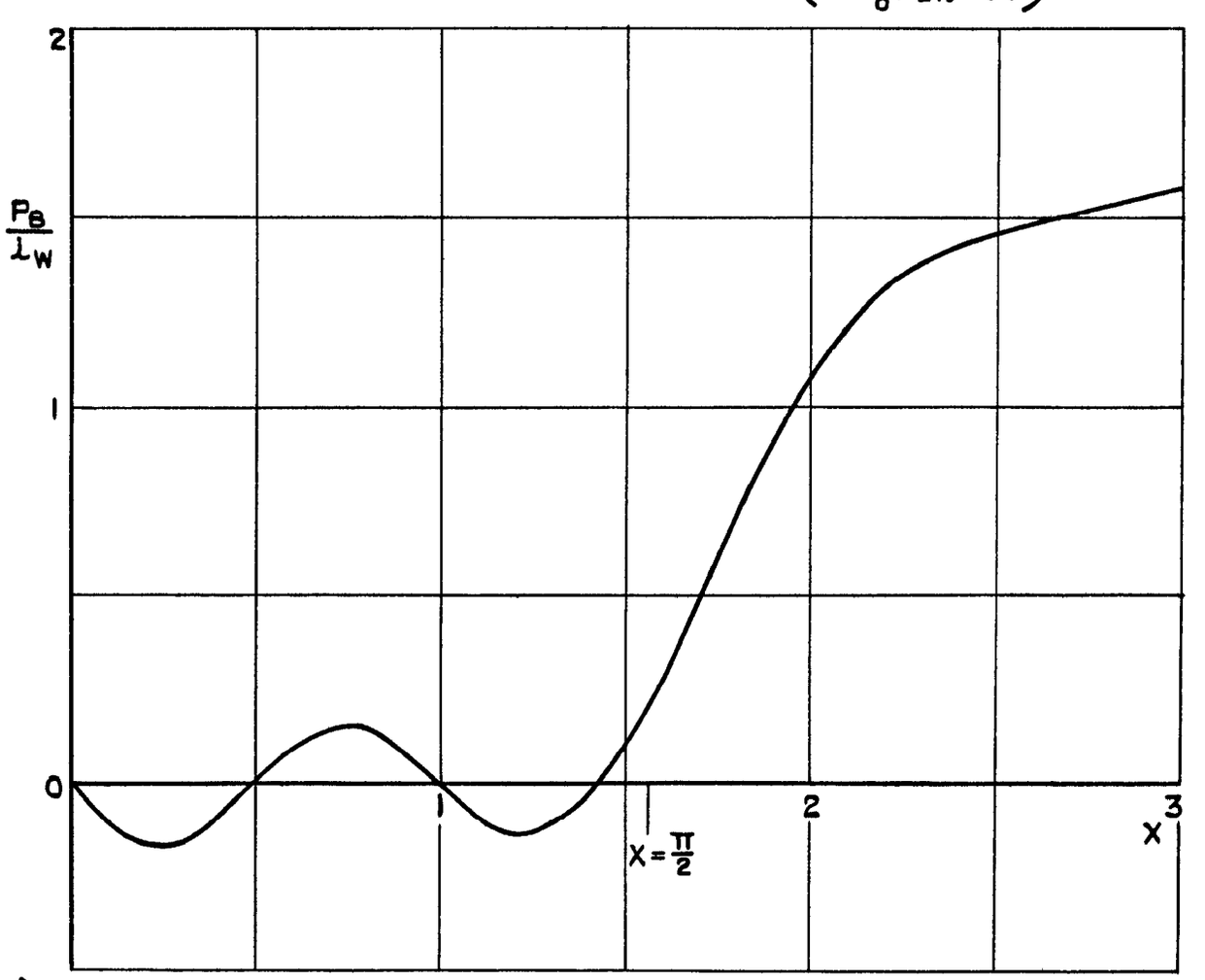


(b) APPROXIMATE PRESSURE ON TOP GENERATOR $(\theta=\frac{\pi}{2})$ GIVEN BY FIRST FOUR FOURIER COMPONENTS $\left(-2\sum_{0}^{3} p_{2n}(X)\cos 2n\frac{\pi}{2}\right)$

FIG. 5 (a&b) APPROXIMATE PRESSURES ON CYLINDRICAL BODY IN COMBINATION WITH WEDGE WING.

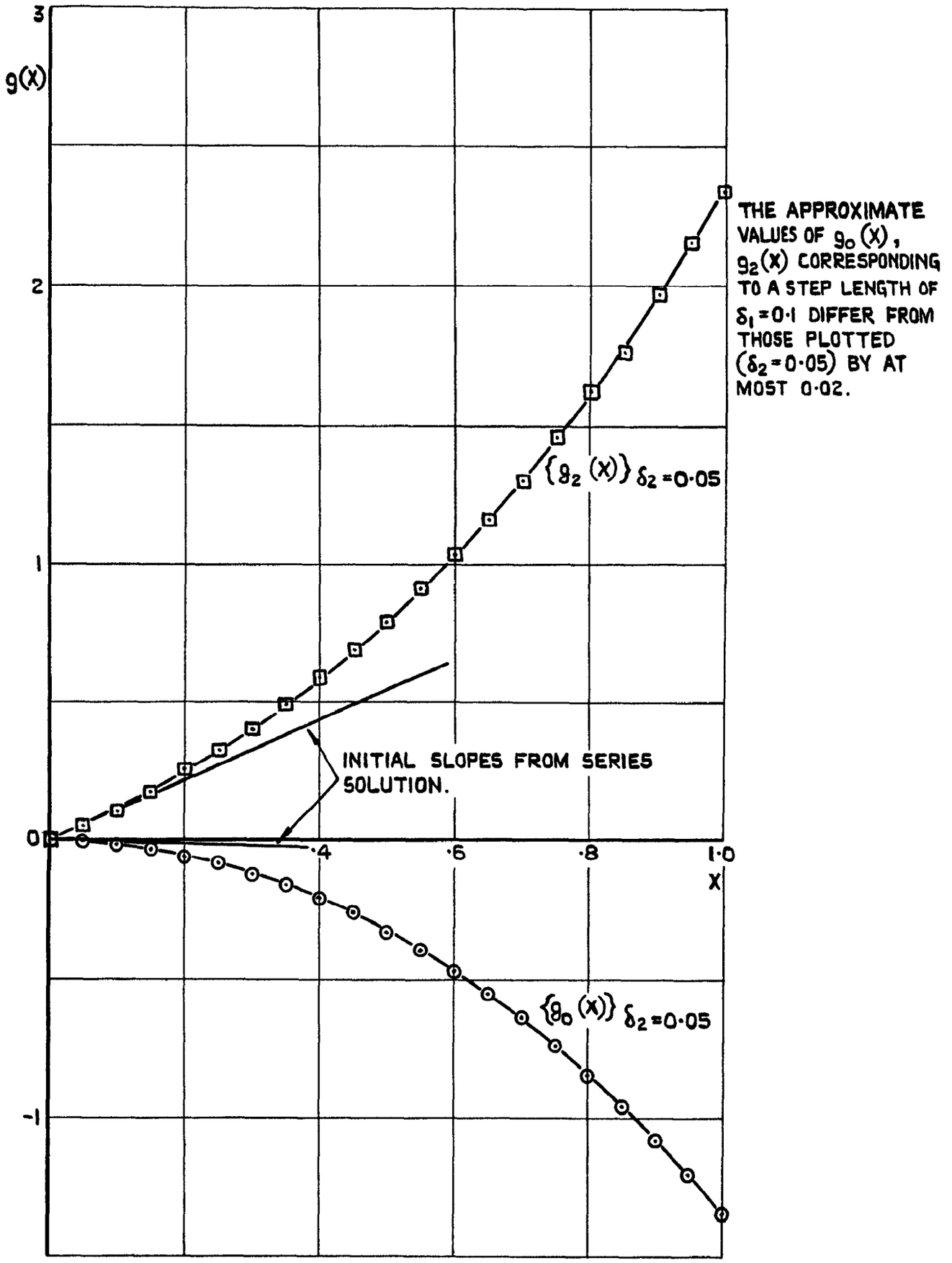


FIG. 6 SOLUTION FOR BODY SHAPE: STEP BY STEP AND SERIES SOLUTIONS.

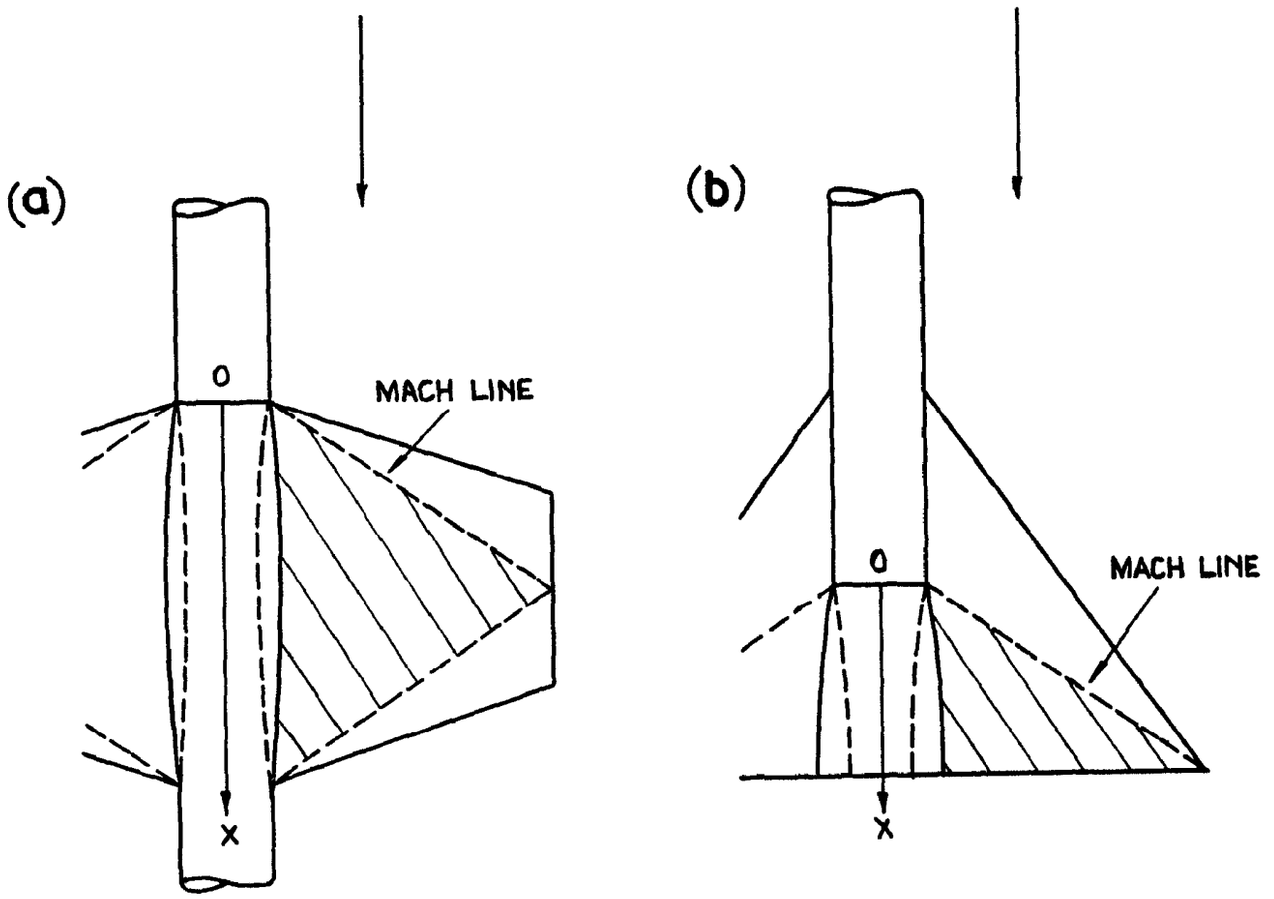


THE UPPER AND LOWER HALVES OF THE FLOW FIELD DUE TO SHAPING ARE INDEPENDENT IN THE SHADED REGIONS.

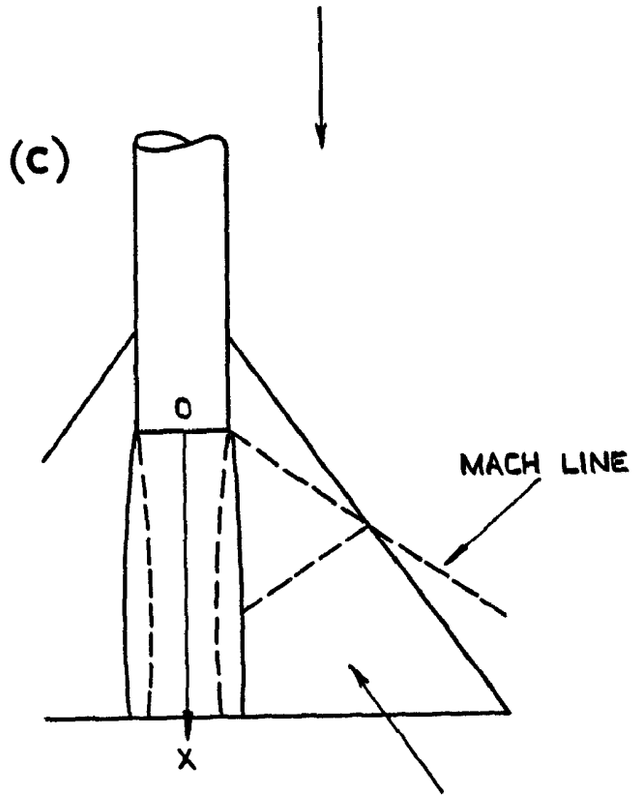


THE UPPER AND LOWER HALVES OF THE FLOW FIELD DUE TO SHAPING ARE NOT INDEPENDENT IN THIS REGION.

FIG. 7 (a - c) COMBINATIONS WITH ANTISYMMETRIC BODY SHAPING.

C.P. No.540

533.695.12:
533.69.048.2:
533.696:
533.6.011.5

A METHOD FOR DESIGNING BODY SHAPE TO PRODUCE PRESCRIBED PRESSURE DISTRIBUTIONS ON WING-BODY COMBINATIONS AT SUPERSONIC SPEEDS. 1.7.1.1.1
1.2.2.6.4
Jones, J. G. April, 1959. 1.3.2

This note presents a numerical method, based on linearised quasi-cylinder theory, for designing body shape to produce prescribed pressures on body and wing in supersonic flow.

C.P. No.540

533.695.12
533.69.048.2:
533.696:
533.6.011.5

A METHOD FOR DESIGNING BODY SHAPE TO PRODUCE PRESCRIBED PRESSUPE DISTRIBUTIONS ON WING BODY COMBINATIONS AT SUPERSONIC SPEEDS. 1.7.1.1.1
1.2.2.6.4
Jones, J. G. April, 1959. 1.3.2

This note presents a numerical method, based on linearised quasi-cylinder theory, for designing body shape to produce prescribed pressures on body and wing in supersonic flow.

C.P. No.540

533.695.12:
533.69.048.2:
533.696:
533.6.011.5

A METHOD FOR DESIGNING BODY SHAPE TO PRODUCE PRESCRIBED PRESSURE DISTRIBUTIONS ON WING-BODY COMBINATIONS AT SUPERSONIC SPEEDS 1.7.1.1.1
1.2.2.6.4
Jones, J.G. April, 1959. 1.3.2

This note presents a numerical method, based on linearised quasi-cylinder theory, for designing body shape to produce prescribed pressures on body and wing in supersonic flow.

Published by
HER MAJESTY'S STATIONERY OFFICE

To be purchased from
York House, Kingsway, London w.c.2
423 Oxford Street, London w.1
13A Castle Street, Edinburgh 2
109 St. Mary Street, Cardiff
39 King Street, Manchester 2
50 Fairfax Street, Bristol 1
2 Edmund Street, Birmingham 3
80 Chichester Street, Belfast 1
or through any bookseller

*Printed in England*

S.O. CODE No.23-9012-40